J. Fluid Mech. (1987), *vol.* 174, *pp.* 23–37
Printed in Great Britain

A numerical solution of the second-order wave-diffraction problem for a submerged cylinder of arbitrary shape

By TORGEIR VADA
A.S. Veritas Research, P.O. Box 300, N-1322 Hovik, Norway

(Received 4 February 1986)

The first- and second-order wave-diffraction problems are solved for a submerged cylinder of arbitrary shape by the integral-equation method based on Green's theorem. The integral equation is solved by an element method using cubic splines. The first- and second-order force components, transmission and reflection coefficients are presented for two different contours. The results for the circular contour are compared with experimental results.

1. Introduction

Two-dimensional, linear radiation and diffraction problems for submerged or semi-submerged bodies have been studied by many authors, and using a variety of numerical methods. Several remarkable results have been found. One of the most interesting is that the reflection coefficient of a submerged, circular cylinder is zero. This was first discovered by Dean (1948) and has been confirmed by all later studies on the problem.

Dean's method, based on the use of a conformal mapping, is not suitable if a complete solution of the problem is wanted. The first complete solution was given by Ursell (1950). He used the multipole method, and his solution was extended to some related problems by Ogilvie (1963). Ogilvie also computed the mean second-order force.

While the radiation problem has been solved for contours of many different shapes, such studies are almost absent for diffraction problems. Some effort has been made by e.g. Leppington & Siew (1980) and Grue & Palm (1984) but the additional assumption that the cylinder is deeply submerged is made in both cases.

A fully nonlinear solution of the diffraction problem is given by Brevig, Greenhow & Vinje (1981). However the steady-state problem is better solved by a perturbation method. This has been done for the radiation problem for a semi-submerged body by several authors. Papanikolaou (1984) has developed a method for solving the complete second-order problem for semi-submerged bodies which is very similar to that used here. However, so far a detailed study of the second-order diffraction problem for submerged bodies, including computation of the resulting wavefield has not, to our knowledge, been given.

An extensive experimental study of the restrained, circular cylinder has been made by Chaplin (1981, 1984*(a, b)*). He has studied the flow field and pressure distribution around the cylinder and has measured the different force components on the cylinder. His work shows that nonlinear effects can be important. This was also found by Longuet-Higgins (1977) in a study on a similar problem.

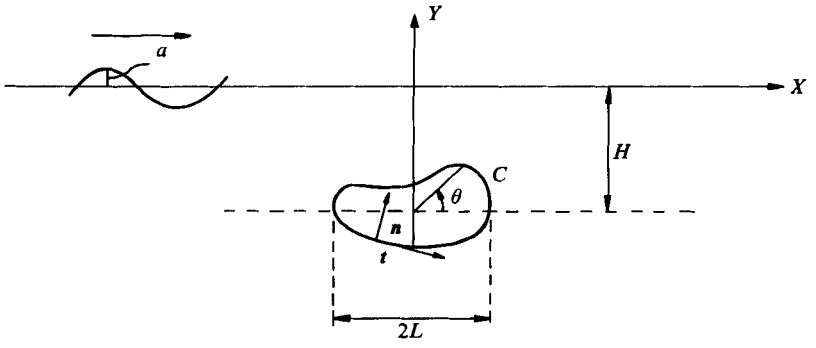

FIGURE 1. Diagram showing the formulation of the problem.

Because of this background we wanted to solve numerically the second-order diffraction problem for a submerged cylinder of arbitrary shape. We have done this by applying the integral-equation method based on Green's theorem, which is chosen because it can be easily applied for contours of arbitrary shape. The integral equation is solved by the collocation method, with the solution expressed as a cubic spline. These polynomials are chosen because of their superior convergence properties compared with the more common choice of constant or linear polynomials. By this method we have been able to compute the second-order force and the second-order reflection and transmission coefficients. The results for two different contours are presented and they clearly show that second-order effects can be important. A comparison with Chaplin's experiments shows a reasonable agreement.

2. Formulation of the problem

A two-dimensional periodic wave with amplitude a and frequency ω is scattered by a submerged cylinder with contour C and its axis parallel to the wave crests (cf. figure 1). The fluid is assumed to be incompressible and the motion is assumed to be irrotational. A velocity potential $\hat{\Phi}$ satisfying the Laplace equation then exists.

The kinematic and dynamic boundary conditions on the free surface are

$$\hat{\eta}_t(X,t)+\hat{\Phi}_x(X,\hat{\eta},t)\,\hat{\eta}_x(X,t)=\hat{\Phi}_y(X,\hat{\eta},t), \tag{2.1}$$

$$-g\hat{\eta}(X,t)=\hat{\Phi}_t(X,\hat{\eta},t)+\tfrac{1}{2}(\nabla\hat{\Phi}(X,\hat{\eta},t))^2. \tag{2.2}$$

We also assume that the cylinder is restrained and that the depth is infinite. This gives the additional conditions

$$\hat{\Phi}=0, \quad Y=-\infty, \tag{2.3}$$

$$\hat{\Phi}_n=0, \quad (X,Y)\in C. \tag{2.4}$$

We now introduce the dimensionless quantities

$$\left.\begin{aligned} &x=\frac{X}{L}, \quad y=\frac{Y}{L}, \quad \epsilon=\frac{a}{L}, \quad h=\frac{H}{L}, \quad K=\frac{L\omega^2}{g},\\ &\tau=\omega t, \quad \eta(x,\tau)=\frac{\hat{\eta}(X,t)}{L}, \quad \Phi(x,y,\tau)=\frac{\hat{\Phi}(X,Y,t)}{\omega L^2},\\ &p(x,y,t)=\frac{\hat{p}(X,Y,t)}{\rho g L}, \quad F(\tau)=\frac{F(t)}{\rho g L^2}, \quad M(\tau)=\frac{\hat{M}(t)}{\rho g L^3}, \end{aligned}\right\} \tag{2.5}$$

where M is the moment with respect to the point $x = 0$, $y = -h$ and $\boldsymbol{F}$ is the force per unit length of the cylinder.

Consistent with the assumption that viscous effects can be neglected, we assume that ϵ is small and expand the potential $\boldsymbol{\Phi}$ in a series

$$\boldsymbol{\Phi} = \sum_{n=1}^{\infty} \epsilon^n \boldsymbol{\Phi}^{(n)}. \tag{2.6}$$

Since the motion is periodic we may write

$$\boldsymbol{\Phi}^{(1)} = \mathrm{Re}\{(\phi_0(x,y)+\phi_7(x,y))\, \mathrm{e}^{-\mathrm{j}\tau}\}, \tag{2.7}$$

$$\boldsymbol{\Phi}^{(2)} = \mathrm{Re}\{\phi_{20}(x,y)+\phi_{22}(x,y)\, \mathrm{e}^{-2\mathrm{j}\tau}\}, \tag{2.8}$$

where j is the imaginary unit and

$$\phi_0(x,y) = -\frac{1}{K}\, \mathrm{e}^{Ky}\, \mathrm{e}^{\mathrm{j}Kx} \tag{2.9}$$

is the potential of the incoming wave. This potential is correct to third order in ϵ because the inhomogeneous terms in the equations for the second- and third-order potentials disappear thereby making these two terms zero. ϕ_7, ϕ_{20} and ϕ_{22} are scattering potentials due to the presence of the cylinder.

The time-independent part of the second-order potential, ϕ_{20}, must probably be found by a different type of method than the one used in this paper. It is also clear from the Bernoulli equation that it will only give a third-order contribution to the force. For these reasons this potential is neglected.

We now introduce the quantities defined in (2.5)–(2.8) into the boundary conditions (2.1)–(2.4), expand (2.1) and (2.2) in a Taylor-series around $y = 0$ and eliminate η. This gives the following boundary conditions for the potentials ϕ_7 and ϕ_{22}:

$$(\phi_7)_n = -(\phi_0)_n, \quad (x,y) \in C, \tag{2.10a}$$

$$(\phi_7)_y - K\phi_7 = 0, \quad y = 0, \tag{2.10b}$$

$$(\phi_7)_y = 0, \quad y = -\infty; \tag{2.10c}$$

$$(\phi_{22})_n = 0, \quad (x,y) \in C, \tag{2.11a}$$

$$(\phi_{22})_y - 4K\phi_{22} = f(x), \quad y = 0, \tag{2.11b}$$

$$(\phi_{22})_y = 0, \quad y = -\infty; \tag{2.11c}$$

where

$$f(x) = \tfrac{1}{2}K\mathrm{j}\,[3K^2(\phi^{(1)})^2 + \phi^{(1)}_{xx}\,\phi^{(1)} + 2(\phi^{(1)}_x)^2]_{y=0} \tag{2.12}$$

and

$$\phi^{(1)} = \phi_0 + \phi_7. \tag{2.13}$$

In addition the potentials must satisfy the Laplace equation and radiation conditions at $x = \pm\infty$. The radiation condition for ϕ_7 is

$$(\phi_7)_x \mp \mathrm{j}K\phi_7 = 0, \quad x = \pm\infty, \tag{2.14}$$

stating that the potential should be an outgoing wave at infinity. From (2.14) and (2.12) we get

$$\lim_{x\to\infty} f(x) = 0, \quad \lim_{x\to-\infty} f(x) = -4K\mathrm{j}R_1, \tag{2.15}$$

where R_1 is the first-order reflection coefficient. Together with (2.11b) this indicates that ϕ_{22} may be written as

$$\phi_{22} = \phi_w + \phi_R,$$

where ϕ_w is a free outgoing wave with frequency 2ω. Hence

$$(\phi_w)_x \mp 4\mathrm{j}K\phi_w = 0, \quad x = \pm\infty,$$

and the remaining part ϕ_R satisfies

$$\phi_R = 0, \quad x = \infty,$$

$$\phi_R = \mathrm{j}R_1, \quad x = -\infty.$$

This gives the following radiation conditions for ϕ_{22}:

$$(\phi_{22})_x - 4\mathrm{j}K\phi_{22} = 0, \quad x = \infty, \tag{2.16}$$

$$(\phi_{22})_x + 4\mathrm{j}K\phi_{22} = -4KR_1, \quad x = -\infty. \tag{2.17}$$

Papanikolaou (1984) does not include the inhomogeneous term in the condition at $x = -\infty$. As we shall see later, this will cause problems in the free-surface integral which appears in the equation for the second-order potential.

The time-dependence of the pressure, force, moment and free-surface elevation is separated out in the same way as for the potential. From the Bernoulli equation we obtain

$$p_1(x, y) = K\mathrm{j}\phi^{(1)}, \tag{2.18}$$

$$p_{20}(x, y) = -\tfrac{1}{4}K\phi_s^{(1)}\overline{\phi_s^{(1)}}, \tag{2.19}$$

$$p_{22}(x, y) = 2K\mathrm{j}\phi_{22} - \tfrac{1}{4}K(\phi_s^{(1)})^2, \tag{2.20}$$

where p_1 is the first-order pressure, p_{20} is the time-independent and p_{22} the oscillatory part of the second-order pressure. The tangential coordinate, s, is increasing in the counterclockwise direction (cf. figure 1). The corresponding components of the force and moment are found by integration of the pressure components around the contour.

The surface elevation is found from the dynamic boundary condition (2.2) which gives

$$\eta_1(x) = K\mathrm{j}\phi^{(1)}(x, 0), \tag{2.21}$$

$$\eta_{20}(x) = \tfrac{1}{4}K(K^2\phi^{(1)}\overline{\phi^{(1)}} - \phi_x^{(1)}\overline{\phi_x^{(1)}})|_{y=0}, \tag{2.22}$$

$$\eta_{22}(x) = K(2\mathrm{j}\phi_{22} - \tfrac{3}{4}K^2(\phi^{(1)})^2 - \tfrac{1}{4}(\phi_x^{(1)})^2)|_{y=0}. \tag{2.23}$$

For the component η_{22} we obtain

$$\eta_{22}(x) = T_2\,\mathrm{e}^{\mathrm{j}4Kx} - \tfrac{1}{2}KT_1^2\,\mathrm{e}^{\mathrm{j}2Kx}, \quad x \to \infty \tag{2.24}$$

$$\eta_{22}(x) = R_2\,\mathrm{e}^{-\mathrm{j}4Kx} - \tfrac{1}{2}K\,\mathrm{e}^{\mathrm{j}2Kx} - \tfrac{1}{2}R_1^2K\,\mathrm{e}^{-\mathrm{j}2Kx}, \quad x \to -\infty \tag{2.25}$$

We notice that the cross-coupling terms between ϕ_0 and ϕ_7 exactly cancel the constant term in ϕ_{22} and hence for $x = -\infty$ the time-dependent part of η consists of one incoming and one outgoing wave with frequency ω and one outgoing wave with frequency 2ω. We define the second-order reflection and transmission coefficients T_2 and R_2 as the (normalized) amplitude of the free wave.

Our aim is now to compute the force, moment, reflection and transmission coefficients.

3. The solution method

3.1. *The first-order problem*

When the Green's function given by Wehausen & Laitone (1960),

$$G(z, \zeta; K) = \mathrm{Re}\left\{\ln(z-\zeta) - \ln(z-\bar{\zeta}) + 2\int_0^\infty \frac{\mathrm{e}^{-\mathrm{i}\nu(z-\bar{\zeta})}}{K-\nu}\,\mathrm{d}\nu - 2\pi\mathrm{j}\,\mathrm{e}^{-\mathrm{i}K(z-\bar{\zeta})}\right\}, \tag{3.1}$$

and the boundary conditions (2.10) and (2.14) are used we obtain an integral equation for the potential ϕ_7 from Green's theorem. The equation is

$$-\pi\phi_7(\hat{s})+\int_C \phi_7(s)\frac{\partial G(s,\hat{s};K)}{\partial n(s)}\,\mathrm{d}s=\int_C -\frac{\partial\phi_0(s)}{\partial n(s)}G(s,\hat{s};K)\,\mathrm{d}s. \tag{3.2}$$

We assume that the contour C can be described by the parametric equations (cf. figure 1)

$$x=x(\theta),\quad y=y(\theta),\quad \theta\in[0,2\pi]. \tag{3.3}$$

This restricts the shape of the body slightly, but should include almost all shapes of practical interest. We apply the relation

$$\mathrm{d}s=A(\theta)\,\mathrm{d}\theta,$$

where

$$A(\theta)=[(x')^2+(y')^2]^{\frac{1}{2}}, \tag{3.4}$$

which brings the integral equation (3.1) to the more convenient form

$$-\pi\phi_7(\hat{\theta})+\int_0^{2\pi}\phi_7(\hat{\theta})\frac{\partial G(\theta,\hat{\theta};K)}{\partial n(\theta)}A(\theta)\,\mathrm{d}\theta=\int_0^{2\pi}-\frac{\partial\phi_0(\theta)}{\partial n(\theta)}G(\theta,\hat{\theta};K)A(\theta)\,\mathrm{d}\theta. \tag{3.5}$$

We now write the solution ϕ_7 as

$$\phi_7(\theta)=\sum_{i=1}^{N}q_iB_i(\theta) \tag{3.6}$$

on C. Here B_i is the cubic spline which is non-zero on the interval $[\theta_{i-2},\theta_{i+2}]$ and we define

$$\theta_0=0,\quad \theta_N=2\pi,\quad \theta_{i\pm N}=\theta_i\pm 2\pi. \tag{3.7}$$

ϕ_7 will now be a piecewise cubic polynomial with two continuous derivatives, hence the velocity has one continuous derivative. Since it is unreasonable to impose a velocity that is smoother than the contour, we also assume that the parametric equations (3.3) have one continuous derivative. If this smoothness condition is not satisfied a modification of the splines must be used (see de Boor 1978).

We now put (3.6) into (3.5) and require that the equation should be exactly satisfied at the points θ_i, $i=1,\ldots,N$. This gives the N equations

$$-\pi(B_{i-1}(\theta_i)q_{i-1}+B_i(\theta_i)q_i+B_{i+1}(\theta_i)q_{i+1})+\sum_{j=1}^{N}A_{ij}q_j=\sum_{j=1}^{N}B_{ij},\quad (i=1,2,\ldots,N), \tag{3.8}$$

where

$$A_{ij}=\int_{\theta_{j-2}}^{\theta_{j+2}}B_j(\theta)\frac{\partial G(\theta,\theta_i;K)}{\partial n(\theta)}A(\theta)\,\mathrm{d}\theta,$$

$$B_{ij}=\int_{\theta_{j-1}}^{\theta_j}-\frac{\partial\phi_0(\theta)}{\partial n(\theta)}G(\theta,\theta_i;K)A(\theta)\,\mathrm{d}\theta,$$

and we assume

$$q_{i\pm N}=q_i, \tag{3.9}$$

which is equivalent to the zero-circulation condition

$$\phi_7(\theta+2\pi)=\phi_7(\theta).$$

The integrals are computed by the three-point Gauss formula on each interval $\langle\theta_{j-1},\theta_j\rangle$, a method which is both computationally efficient and sufficiently accurate.

When this system is solved, ϕ_7 is known on C from (3.6) and the first-order and mean pressure can be found from (2.18) and (2.19). The corresponding components of the force and moment can then be found by integration around the contour.

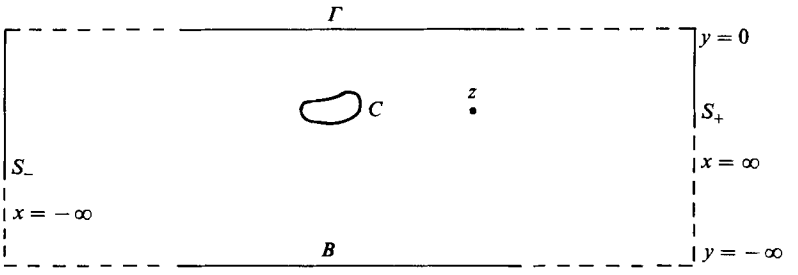

FIGURE 2. The integration limits.

When the potential is known on the contour it can be found anywhere else from Green's theorem:

$$\phi_7(z) = \frac{1}{2\pi}\int_0^{2\pi}\left(\frac{\partial\phi_0(\theta)}{\partial n(\theta)}\,G(z,\zeta(\theta);K)+\phi_7(\theta)\,\frac{G(z,\zeta(\theta);K)}{\partial n(\theta)}\right)A(\theta)\,\mathrm{d}\theta. \tag{3.10}$$

Now with $z = x$ we can find the surface elevation $\eta_1(x)$ from (2.21), and after differentiation of (3.10) with respect to x we can find $(\phi_7)_x(x,0)$ and thereby $\eta_{20}(x)$ from (2.22).

3.2. *The second-order problem*

An integral equation for ϕ_{22} is obtained in the same way as for ϕ_7. We use Green's theorem and the Green's function (3.1) with K replaced by $4K$.

When the boundary conditions (2.11), (2.16) and (2.17) are used the integrals over B and S_+ (cf. figure 2) vanish and we obtain

$$-2\pi\phi_{22}(z) = \int_C -\phi_{22}(s)\,\frac{\partial G(z,\zeta(s);4K)}{\partial n(s)}\,\mathrm{d}s + \int_\Gamma f(\xi)\,G(z,\xi;4K)\,\mathrm{d}\xi + \int_{S_-} 4KR_1\,G(z,\zeta(s);4K)\,\mathrm{d}s,$$

where the function $f(\xi)$ is defined in (2.12). This function is computed using (3.10) and the two first derivatives of (3.10) with respect to x. This avoids the loss of accuracy that would result if numerical derivatives were used.

The free-surface integral is truncated by setting

$$\int_\Gamma f(\xi)\,G(z,\xi;4K)\,\mathrm{d}\xi \approx \int_{x_L}^{x_R} f(\xi)\,G(z,\xi;4K)\,\mathrm{d}\xi,$$

where x_R is chosen so large that $f(\xi)$ is sufficiently small for all $\xi > x_R$, and x_L (< 0) must be sufficiently large in value that

$$f(\xi) \approx -4K\mathrm{j}R_1 \qquad (\forall\xi < x_L),$$

$$G(z,\zeta;4K) \approx \alpha(z)\,\mathrm{e}^{-4\mathrm{j}K\xi}\,\mathrm{e}^{4K\eta} \qquad (\forall\xi < x_L).$$

Substituting the angle θ for s we then have

$$-2\pi\phi_{22}(z) = \int_0^{2\pi} -\phi_{22}(\theta)\,\frac{\partial G(z,\zeta;4K)}{\partial n(\theta)}\,A(\theta)\,\mathrm{d}\theta + \int_{x_L}^{x_R} f(\xi)\,G(z,\zeta;4K)\,\mathrm{d}\xi + R_1\,G(z,x_L;4K). \tag{3.11}$$

Letting $z \to x(\hat{\theta}) + \mathrm{i}y(\hat{\theta})$ we now obtain the integral equation for ϕ_{22}:

$$-\pi\phi_{22}(\hat{\theta}) + \int_0^{2\pi} \phi_{22}(\theta) \frac{\partial G(\hat{\theta}, \theta; 4K)}{\partial n(\theta)} A(\theta)\,\mathrm{d}\theta$$

$$= \int_{\xi_L}^{\xi_R} f(\xi)\, G(z(\hat{\theta}), \xi; 4K)\,\mathrm{d}\xi + R_1\, G(z(\hat{\theta}), x_L; 4K). \quad (3.12)$$

Provided that x_L is sufficiently large in value, the expression on the right-hand side will be independent of the actual choice of x_L. The integral is computed by the midpoint rule. Papanikolaou (1984) met problems here because of the inaccurate radiation condition, as mentioned in §2. He does not include the last term, which is the contribution from S_-. Hence there is no term which counteracts the oscillatory behaviour of the integrand.

This equation is solved in exactly the same way as the first-order equation. We write ϕ_{22} as the piecewise cubic polynomial

$$\phi_{22} = \sum_{i=1}^{N} \gamma_i B_i(\theta), \quad (3.13)$$

where γ_i is the solution of the linear equations

$$-\pi(B_{i-1}(\theta_i)\gamma_{i-1} + B_i(\theta_i)\gamma_i + B_{i+1}(\theta_i)\gamma_{i+1}) + \sum_{j=1}^{N} C_{ij}\gamma_j = D_i \quad (i = 1, 2, \ldots, N), \quad (3.14)$$

with

$$C_{ij} = \int_{\theta_{j-2}}^{\theta_{j+2}} B_j(\theta) \frac{\partial G(\theta_i, \theta; 4K)}{\partial n(\theta)} A(\theta)\,\mathrm{d}\theta,$$

$$D_i = \int_{x_L}^{x_R} f(\xi)\, G(z(\theta_i), \xi; 4K)\,\mathrm{d}\xi + R_1\, G(z(\theta_i), x_L; 4K),$$

and the zero circulation (periodicity) condition

$$\gamma_{i \pm N} = \gamma_i$$

is imposed.

When (3.14) is solved ϕ_{22} is known on C from (3.13) and the second-order oscillatory pressure component, p_{22} can be found from (2.20). The corresponding components of the force and moment can be found by integration.

From (3.11) ϕ_{22} can be found anywhere in the fluid when it is known on C. In particular $\phi_{22}(x, 0)$ can be found, and hence η_{22} can be computed from (2.23).

3.3. *Numerical accuracy and convergence*

In our calculations we wanted an accuracy of 0.01 or less. This was achieved by using 20–25 elements if some care was taken when the elements were distributed around the contour. The left boundary (i.e. x_L) had to be somewhere between $x = -5$ and -8 depending on the wavenumber, whereas the right boundary (x_R) never had to be further out than $x = 6$.

In the Appendix an alternative calculation method for the second-order force is described. This gives a valuable check of the accuracy.

A comparison with linear elements clearly shows the superiority of higher-order polynomials. The first-order problem can be solved with good accuracy with only 11 cubic elements. For a long wave ($K = 0.5$) this gave at least as good accuracy as we obtained with 130 linear elements, and the computation time was reduced by a factor of 80. This indicates that the introduction of higher-order polynomials is almost a

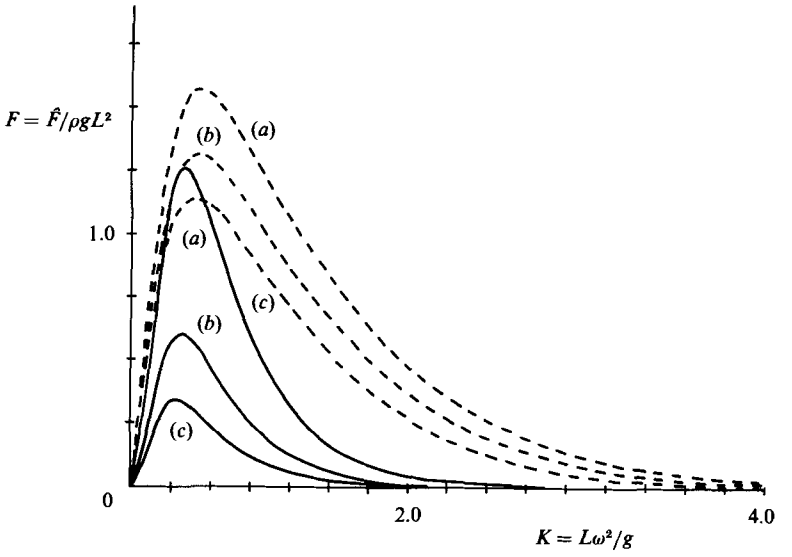

FIGURE 3. First- and second-order oscillatory force on the circle. (*a*) $h = 1.5$; (*b*) 1.75; (*c*) 2.0; – – –, $|F_1 \cdot i| = |F_1 \cdot j|$; ——, $|F_{22} \cdot i| = |F_{22} \cdot j|$.

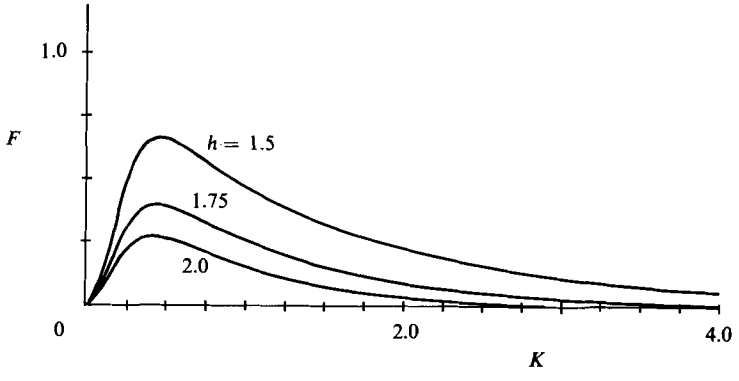

FIGURE 4. Mean vertical force on the circle.

necessity for the solution of the second-order problem. In this respect the problem with the submerged body differs from the problem with the semi-submerged body, where constant or linear elements seem to give sufficient accuracy. This is probably because the flow in the narrow region between the body and the free surface is too complicated to be described sufficiently accurately, with a reasonable number of elements, by the lower-order polynomials.

4. Numerical results

We have applied the theory described in this paper to several contours described by the equations

$$x = \frac{\cos\theta - \alpha\cos 3\theta}{1-a}, \quad y = b\frac{\sin\theta + \alpha\sin 3\theta}{1-\alpha}$$

and we here present the results for the two cases $\alpha = 0$, $b = 1$ which gives a circle, and $\alpha = 0.1$, $b = 0.5$ which gives the following pontoon-like contour:

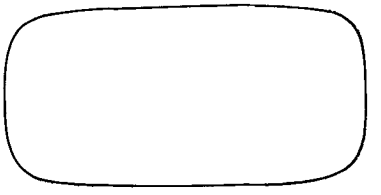

4.1. *The force and moment*

The first- and second-order oscillatory force components are shown in figure 3. It is clear from this figure that the second-order component can be quite important for the long waves when the cylinder is close to the free surface. However, the second-order component decreases much more rapidly than the first-order component when the wavenumber increases beyond the maximum point or the cylinder is moved away from the free surface.

The mean vertical force on the circle is shown in figure 4. It is seen to be quite significant even for fairly large wavenumbers. The force is directed upwards and is due to a lowering of the mean free surface above the cylinder. This effect is discussed in detail in Longuet-Higgins (1977).

Chaplin (1984*b*) has measured the various force components on the circular cylinder. The first-order and mean components agree very well with Ogilvie's (1963) results, which again agree completely with ours. The second-order oscillatory component is compared in table 1. The experimental values given here are valid for Keulegan–Carpenter numbers Kc less than 1 when

$$Kc = \pi\epsilon\, \mathrm{e}^{-Kh}.$$

For larger values of Kc viscous effects become increasingly important.

A comparison between cases I, II and V, VI clearly shows that the variation with h is described very well by our theory. The variation with K, however, is not quite as good. The deviation in case I seems to be due to viscous effects, because if only the measurements for the lowest Kc-values are used a value much closer to ours is obtained. It will not be surprising if viscous effects are more important for this very long wave than in the other cases. The reason for the deviation in case IV is unclear, but it indicates that our theory, for some reason, gives a too rapid decrease of the force with increasing wavenumber.

The oscillatory force components for the pontoon are shown in figures 5 and 6. The values of h are chosen such that the distance from the free surface to the upper point on the cylinder is the same as for the circle. We notice that for this contour there seem to be some wavenumbers for which the force is zero. We also see that the nonlinear effect is much more important for the pontoon than for the circle in the case when the bodies are closest to the free surface, whereas the results become more similar when the bodies are moved away from the free surface. This is not surprising since the actual shape of the body obviously becomes more important when it is close to the free surface. It is also to be expected that the pontoon will have the larger vertical force. However it is somewhat surprising that the horizontal force seems to be more nonlinear than the vertical component.

Another interesting nonlinear effect is shown in figure 7 where the oscillatory components of the moment are plotted. The first-order moment has its maximum

Parameters				
h	K	Case	Theory	Experiment (Chaplin 1984*b*)
2.0	0.206	I	0.31	0.39
2.0	0.365	II	0.33	0.33
2.0	0.570	III	0.21	0.21
2.0	0.821	IV	0.09	0.16
3.0	0.206	V	0.06	0.05
3.0	0.365	VI	0.04	0.05

TABLE 1. Comparison of second-order oscillatory component

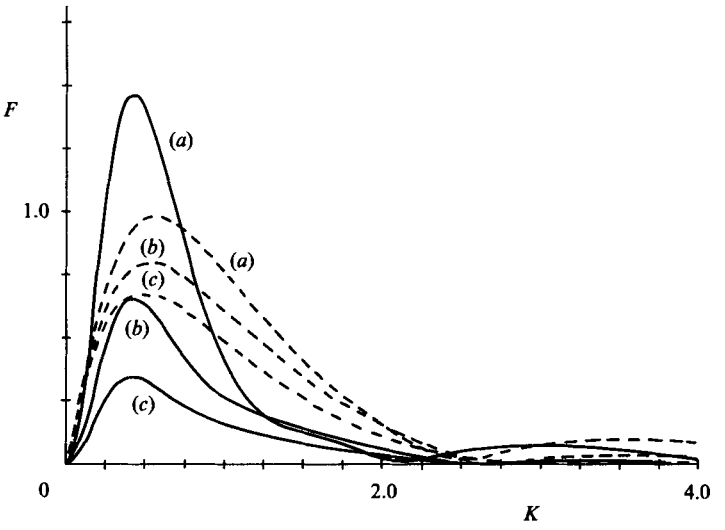

FIGURE 5. First- and second-order horizontal oscillatory forces on the pontoon. (*a*) $h = 1.0$; (*b*) 1.25; (*c*) 1.5; – – –, $|F_1 \cdot i|$; ——, $|F_{22} \cdot i|$.

for wavelengths about twice the length of the body, as one would expect. The second-order moment on the other hand shows a similar behaviour as the forces. This has the consequence that unless ϵ is very small, the second-order component gives the dominant contribution to the moment for the long waves.

The mean vertical force and mean moment are shown in figure 8. The moment is negative, as expected, but it is very small. The force shows the same behaviour as for the circle, but again we get a significantly larger value for the smallest value of h.

4.2. *Transmission and reflection coefficients*

In figure 9 the second-order transmission coefficient for the circle is shown. The result is quite surprising. For the smallest value of h we see that the amplitude of the $4K$-wave can be of the same size as the amplitude of the first harmonic. This results in a transmitted wave like the one shown in figure 10. This very strong nonlinear effect is also immediately observed in a wave tank. Unfortunately there are, as far as we know, no measurements of the amplitude of the second harmonic for the restrained cylinder. Longuet-Higgins (1977) has measured it for a circle that was restrained only in the vertical direction. Since this cylinder will give some reflection of the incoming

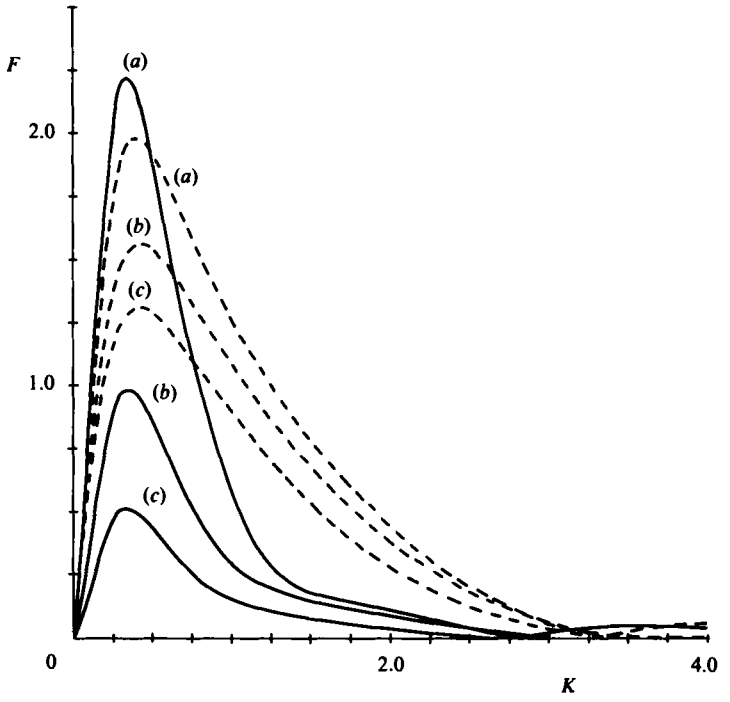

FIGURE 6. First- and second-order vertical oscillatory forces on the pontoon. (*a*) $h = 1.0$; (*b*) 1.25; (*c*) 1.5; – – –, $|F_1 \cdot j|$; ——, $|F_{22} \cdot j|$.

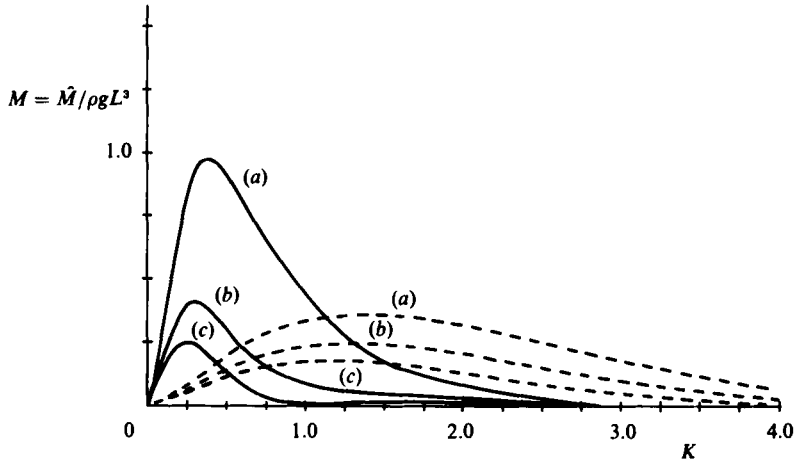

FIGURE 7. First- and second-order oscillatory moment on the pontoon. (*a*) $h = 1.0$; (*b*) 1.25; (*c*) 1.5; – – –, M_1; ——, M_{22}.

wave we would expect the amplitude of the transmitted wave to be somewhat smaller than for the restrained cylinder. For $K = 0.3$, $h = 1.67$ he found $T_2 \approx 1.2$ whereas we obtained $T_2 = 1.85$ for the restrained cylinder with the same values of h and K. The difference is perhaps a bit too big, but we think that this confirms that the results shown here are in reasonable agreement with what actually happens.

As mentioned earlier, $R_1 = 0$ for the circle. We were therefore particularly

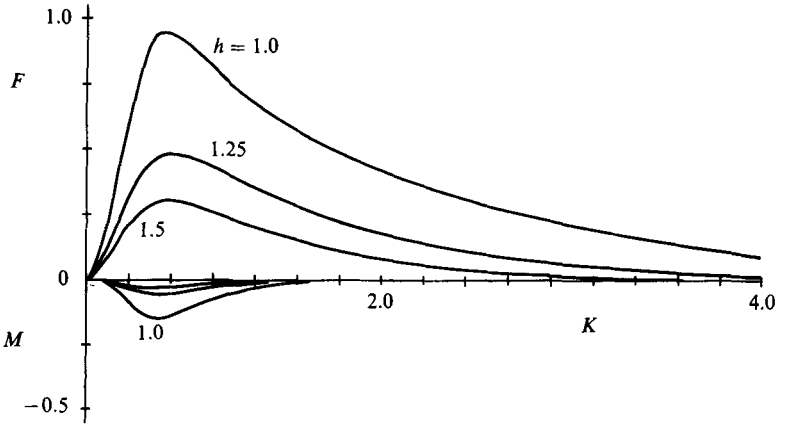

FIGURE 8. Mean vertical force (positive) and mean moment (negative) on the pontoon. The three curves for the moment correspond to the same h-values as the curves for the force.

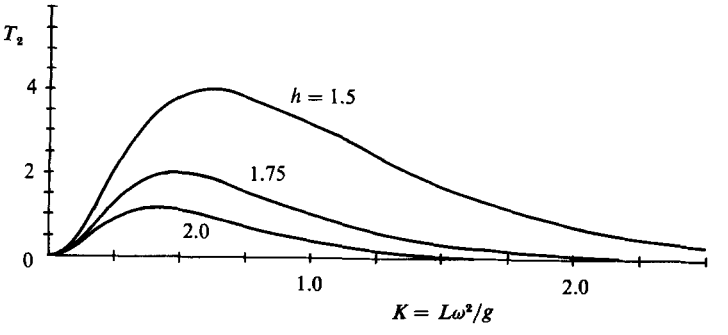

FIGURE 9. Second-order transmission coefficient for the circle ($T_1 = 1.0$).

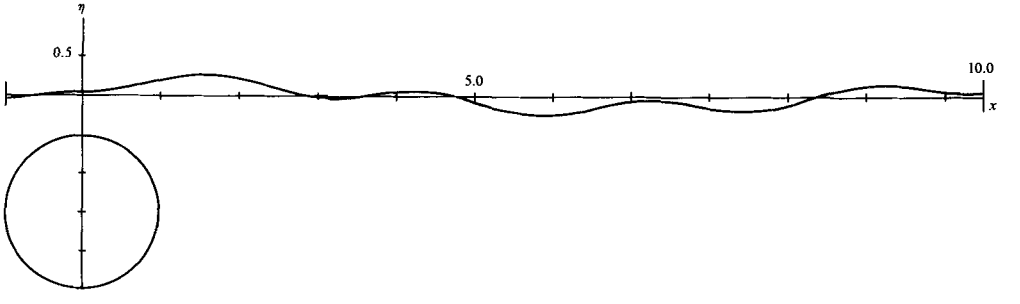

FIGURE 10. The surface elevation in natural scale for $K = 0.56$, $\epsilon = 0.16$, $h = 1.5$, $\tau = 0$.

interested in finding out whether the same was true for the second-order coefficient. In the computation we obtained values of R_2 in the order 0.01. This is of the same size as the estimated numerical accuracy of the method, but the result seems significant as we obtained a smooth sinusoidal behaviour of the potential. Hence we believe that there is a very small reflected second-order wave, but for all practical purposes $R_2 \approx 0$. This is in agreement with the experiments of Chaplin and others.

The second-order transmission coefficient for the pontoon, shown in figure 11, shows the same features as for the circle. Figure 12 shows that the same effect is

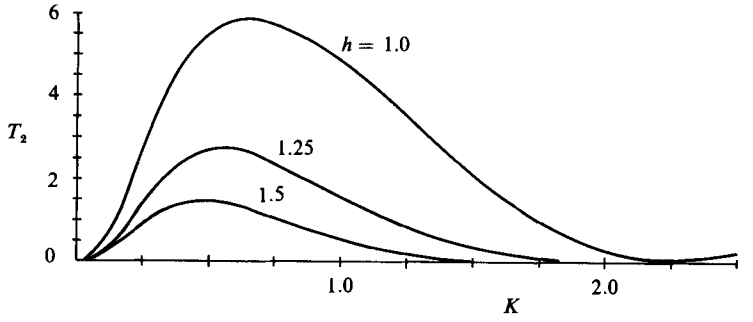

FIGURE 11. Second-order transmission coefficient for the pontoon ($T_1 \approx 1.0$).

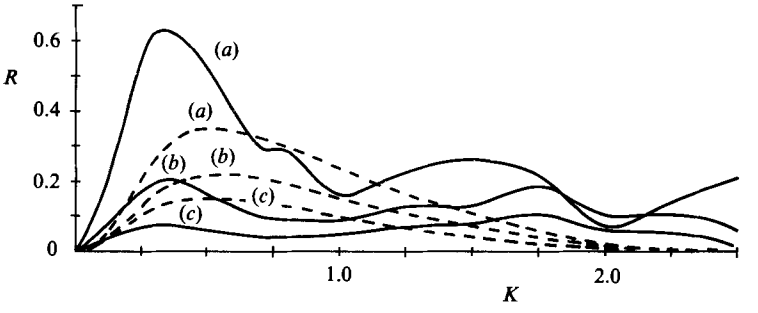

FIGURE 12. First- and second-order reflection coefficients for the pontoon (*a*) $h = 1.0$; (*b*) 1.25; (*c*) 1.5; ——, R_2; – – –, R_1.

present in the reflected wave as well, but it is not quite as dramatic as for the transmitted wave. The maximum value of the first-order reflection coefficient corresponds to a mean horizontal force of 0.065 so this component of the force is always very small.

5. Conclusion

From the results presented in this paper we conclude that second-order effects can be important for cylinders close to the free surface. The effect is most important in the description of the wavefield, but the force may also be significantly affected. From the comparison with Chaplin's experiments we believe that the effect can be obtained with reasonable accuracy by the method presented.

The work on this paper was done as part of my dr.scient studies at the Section for Mechanics, Department of Mathematics, University of Oslo under supervision of Professor Enok Palm, who gave very helpful advice at several stages of the work. I also want to thank John Grue for useful and interesting discussions.

Appendix. An alternative computation of the second-order force

Applying the Haskind relations (cf. Newman 1977) it is possible to compute M_{22} and $\boldsymbol{F}_{22}$ without the solution of the ϕ_{22}-problem. Instead a set of first-order problems must be solved.

If ϕ_i is the first-order radiation potential for an oscillation with frequency 2ω, where

$i = 1, 2, 6$ corresponds to the sway, heave and roll respectively, we get from Green's theorem (cf. figure 2)

$$\int_C \left(\phi_i \frac{\partial \phi_{22}}{\partial n} - \phi_{22} \frac{\partial \phi_i}{\partial n}\right) \mathrm{d}s + \int_\Gamma \phi_i(\xi, 0) f(\xi)\, \mathrm{d}\xi + \int_{S_-} \phi_i\, 4KR_1\, \mathrm{d}s = 0.$$

As in §3 we truncate the integration over Γ by setting

$$\int_\Gamma \phi_i(\xi, 0) f(\xi)\, \mathrm{d}\xi \approx \int_{x_\mathrm{L}}^{x_\mathrm{R}} \phi_i(\xi, 0) f(\xi)\, \mathrm{d}\xi,$$

where $f(\xi)$ is sufficiently small for $\xi > x_\mathrm{R}$ and

$$f(\xi) \approx -4K\mathrm{j}R_1, \quad \phi_i(\xi, 0) \approx A_i\, \mathrm{e}^{-4K\mathrm{j}\xi}\, \mathrm{e}^{4K\eta} \quad \text{for } \xi < x_\mathrm{L}.$$

This gives

$$\int_C \phi_{22} \frac{\partial \phi_i}{\partial n}\, \mathrm{d}s = -\int_{x_\mathrm{L}}^{x_\mathrm{R}} \phi_i(\xi, 0) f(\xi)\, \mathrm{d}\xi - A_i R_1\, \mathrm{e}^{-4K\mathrm{j}x_\mathrm{L}}, \tag{A 1}$$

where the right-hand side is independent of x_L if $|x_\mathrm{L}|$ is sufficiently large. Since

$$(\phi_i)_n = n_i, \quad i = 1, 2,$$

$$(\phi_i)_n = (\boldsymbol{r} \times \boldsymbol{n}) \cdot \boldsymbol{k}, \quad i = 6,$$

we see that the integral of the first term in (2.20) can be calculated by (A 1).

This method has been used in several works on the second-order radiation problems. However, since the solution for the potentials on the free surface is needed, the solution of each of the first-order problems is equally time-consuming as the solution of the second-order problem. Hence, unless these potentials are already known, this method is far more time-consuming than the direct solution of the second-order problem. In addition to this, we wanted to find the second-order surface elevation as well as the force, and for this calculation the second-order potential is needed anyway. For these reasons we have only use this method to check the results for a few sets of the parameters.

REFERENCES

Brevig, P., Greenhow, M. & Vinje, T. 1981 Extreme wave forces on submerged cylinders. *2nd Intl Symp. on Wave and Tidal Energy*, pp. 143–166.

Chaplin, J. R. 1981 On the irrotational flow around a horizontal cylinder in waves. *J. Appl. Mech.* **48**, 689–694.

Chaplin, J. R. 1984*a* Mass transport around a horizontal cylinder beneath waves. *J. Fluid Mech.* **140**, 175–187.

Chaplin, J. R. 1984*b* Nonlinear forces on a horizontal cylinder beneath waves. *J. Fluid Mech.* **147**, 449–464.

Dean, W. R. 1948 On the reflection of surface waves by a submerged circular cylinder. *Proc. Camb. Phil. Soc.* **44**, 483–491.

de Boor, C. 1978 *A Practical Guide to Splines*, pp. 125–126, 299ff. Springer.

Grue, J. & Palm, E. 1984 Reflection of surface waves by submerged cylinders. *Appl. Ocean Res.* **6**, 54–60.

Leppington, F. G. & Siew, P. F. 1980 Scattering of surface waves by a submerged cylinder. *Appl. Ocean Res.* **2**, 129–137.

Longuet-Higgins, M. S. 1977 The mean forces exerted by waves on floating and submerged bodies with applications to sand bars and wave power machines. *Proc. R. Soc. Lond.* A **352**, 463–480.

NEWMAN, J. N. 1977 *Marine Hydrodynamics*, pp. 303–304. MIT Press.

OGILVIE, T. 1963 First- and second-order forces on a cylinder submerged under a free surface. *J. Fluid Mech.* **16**, 451–472.

PAPANIKOLAOU, A. 1984 On calculations of nonlinear hydrodynamic effects in ship motion. *Schiffstechnik* **31**, 89–129.

URSELL, F. 1950 Surface waves on deep water in the presence of a submerged circular cylinder. *Proc. Camb. Phil. Soc.* **46**, 141–158.

WEHAUSEN, J. V. & LAITONE, E. V. 1960 Surface waves. *Handbuch der Physik*, vol. 9, pp. 479–481.